

Clinical Cancer Research



Profiles of Genomic Instability in High-Grade Serous Ovarian Cancer Predict Treatment Outcome

Zhigang C. Wang, Nicolai Juul Birkbak, Aedín C. Culhane, et al.

Clin Cancer Res 2012;18:5806-5815. Published OnlineFirst August 21, 2012.

Updated Version Access the most recent version of this article at:
doi:[10.1158/1078-0432.CCR-12-0857](https://doi.org/10.1158/1078-0432.CCR-12-0857)

Supplementary Material Access the most recent supplemental material at:
<http://clincancerres.aacrjournals.org/content/suppl/2012/08/21/1078-0432.CCR-12-0857.DC1.html>

Cited Articles This article cites 48 articles, 21 of which you can access for free at:
<http://clincancerres.aacrjournals.org/content/18/20/5806.full.html#ref-list-1>

E-mail alerts [Sign up to receive free email-alerts](#) related to this article or journal.

Reprints and Subscriptions To order reprints of this article or to subscribe to the journal, contact the AACR Publications Department at pubs@aacr.org.

Permissions To request permission to re-use all or part of this article, contact the AACR Publications Department at permissions@aacr.org.

Profiles of Genomic Instability in High-Grade Serous Ovarian Cancer Predict Treatment Outcome

Zhigang C. Wang¹, Nicolai Juul Birkbak^{1,6}, Aedin C. Culhane², Ronny Drapkin^{3,4}, Aquila Fatima¹, Ruiyang Tian¹, Matthew Schwede², Kathryn Alsop¹⁰, Kathryn E. Daniels³, Huiying Piao^{3,4}, Joyce Liu³, Dariush Etemadmoghadam^{7,8,9}, Alexander Miron¹, Helga B. Salvesen^{12,13}, Gillian Mitchell¹⁰, Anna DeFazio¹¹, John Quackenbush², Ross S. Berkowitz⁵, J. Dirk Iglehart¹, David D.L. Bowtell^{7,8,9}; for the Australian Ovarian Cancer Study Group, and Ursula A. Matulonis³

Abstract

Purpose: High-grade serous cancer (HGSC) is the most common cancer of the ovary and is characterized by chromosomal instability. Defects in homologous recombination repair (HRR) are associated with genomic instability in HGSC, and are exploited by therapy targeting DNA repair. Defective HRR causes uniparental deletions and loss of heterozygosity (LOH). Our purpose is to profile LOH in HGSC and correlate our findings to clinical outcome, and compare HGSC and high-grade breast cancers.

Experimental Design: We examined LOH and copy number changes using single nucleotide polymorphism array data from three HGSC cohorts and compared results to a cohort of high-grade breast cancers. The LOH profiles in HGSC were matched to chemotherapy resistance and progression-free survival (PFS).

Results: LOH-based clustering divided HGSC into two clusters. The major group displayed extensive LOH and was further divided into two subgroups. The second group contained remarkably less LOH. *BRCA1* promoter methylation was associated with the major group. LOH clusters were reproducible when validated in two independent HGSC datasets. LOH burden in the major cluster of HGSC was similar to triple-negative, and distinct from other high-grade breast cancers. Our analysis revealed an LOH cluster with lower treatment resistance and a significant correlation between LOH burden and PFS.

Conclusions: Separating HGSC by LOH-based clustering produces remarkably stable subgroups in three different cohorts. Patients in the various LOH clusters differed with respect to chemotherapy resistance, and the extent of LOH correlated with PFS. LOH burden may indicate vulnerability to treatment targeting DNA repair, such as PARP1 inhibitors. *Clin Cancer Res*; 18(20); 5806–15. ©2012 AACR.

Introduction

Epithelial cancers of the ovary are a diverse collection of histologically and genetically distinct diseases. Major sub-

types include serous, mucinous, endometrioid, and clear-cell cancers based principally on their microscopic morphology. Genetic and genomic differences support these morphologic distinctions. High-grade serous cancer (HGSC) of the ovary is the most common subtype and is distinguished from other ovarian cancers by aneuploid genomes and a large burden of copy number gains and losses (1, 2). Recently, The Cancer Genome Atlas (TCGA) Research Network explored HGSC using a variety of molecular approaches. Attempts were made to delineate subtypes of HGSC based on transcriptional profiles, methylation, and microRNA expression. miRNA clustering was able to predict overall survival among 487 separate patients. Supervised clustering and modeling mRNA expression data did derive a high-risk signature, which significantly predicted overall survival (3). Molecular subtypes defined by gene expression in the TCGA recapitulated subtypes described by Tothill and colleagues from the Australian Ovarian Cancer Study (AOCS) that are associated with disease outcome (4, 5).

TCGA investigators determined copy number using high-density arrayed genomic probes to assess absolute copy number but not to distinguish gain or loss of parental

Authors' Affiliations: Departments of ¹Cancer Biology, ²Biostatistics and Computational Biology, and ³Medical Oncology, Dana-Farber Cancer Institute; ⁴Department of Pathology and ⁵Division of Gynecologic Oncology, Department of Obstetrics and Gynecology, Brigham and Women's Hospital, Boston, Massachusetts; ⁶Center for Biological Sequence Analysis, Technical University of Denmark, Lyngby, Denmark; ⁷Cancer Genomics Program, Departments of ⁸Biochemistry and ⁹Pathology, and ¹⁰Familial Cancer Centre, Peter MacCallum Cancer Centre and the University of Melbourne, Parkville, Melbourne, Victoria; ¹¹Department of Gynaecological Oncology and Westmead Institute for Cancer Research, University of Sydney at Westmead Millennium Institute, Westmead Hospital, Westmead, New South Wales, Australia; ¹²Department of Obstetrics and Gynecology, Haukeland University Hospital; and ¹³Department of Clinical Medicine, University of Bergen, Bergen, Norway

Note: Supplementary data for this article are available at Clinical Cancer Research Online (<http://clincancerres.aacrjournals.org/>).

Corresponding Authors: J. Dirk Iglehart, Dana-Farber Cancer Institute, 450 Brookline Avenue, Boston, MA 02215. Phone: 617-632-5178; Fax: 617-632-3709; E-mail: jiglehart@partners.org; and Ursula A. Matulonis, Dana-Farber Cancer Institute, 450 Brookline Avenue, Boston, MA 02215. Phone: 617-632-2334; Fax: 617-632-3479; E-mail: umatulonis@partners.org

doi: 10.1158/1078-0432.CCR-12-0857

©2012 American Association for Cancer Research.

Translational Relevance

High-grade serous cancer (HGSC) of the ovary is a highly lethal disease that is frequently characterized by chromosomal instability, defects in homologous recombination repair (HRR), and sensitivity to DNA-damaging agents, especially platinum-based therapies. However, not all HGSC show defects in HRR and currently the ability to predict response to first-line treatment is limited. We show HGSC can be reproducibly separated into groups based on the pattern of LOH, and multivariate analysis finds a subgroup with low chemotherapy resistance. The extent of LOH correlated with progression-free survival. Extensive LOH was also seen in triple-negative breast cancer (TNBC) relative to other breast cancer subtypes. Although some chromosomal regions affected by LOH differed between TNBC and HGSC, finding extensive LOH in both cancers suggests common molecular mechanisms between these diseases. Our findings provide biomarkers of response to treatment in HGSC, which may aid treatment planning with therapies targeting DNA repair, such as PARP1 inhibitors.

alleles. We previously used single nucleotide polymorphism (SNP) arrays to profile allelic imbalance (AI) in breast cancer, and found correlations with subtypes classified by expression of the estrogen receptor (ER), progesterone receptor (PR), and the HER2 receptor-like protein, and by histologic grade (6, 7). ER-positive or HER2-positive breast tumors may derive from luminal epithelial progenitors (luminal breast cancers), whereas tumors negative for ER, PR, and HER2 (triple-negative breast cancer, TNBC) may have a different histogenesis (8–10). TNBCs share features with HGSC. Both TNBC and HGSC frequently have p53 mutations and both display chromosomal instability and are observed in women inheriting a disease-associated mutation in BRCA1 (3, 9, 11–13). Platinum-containing drugs are very active in ovarian cancer, particularly in HGSC, and platinum drugs alone or in combination have been used successfully in TNBC (14–18). Finally, the genomes of sporadic HGSC and TNBC harbor common loss of single parental alleles, detected as LOH or AI, within or encompassing whole chromosomes (6, 7, 19, 20). We reasoned that the burden and pattern of AI may distinguish subtypes of HGSC, and genomic subtypes might predict response to initial treatment as well as overall survival. Analysis of AI in HGSC may also provide further insights into molecular relationships with TNBC.

We conducted SNP arrays in HGSC from patients presenting for treatment in Boston, MA, USA, and validated our results in 2 independent cohorts of HGSC. Hierarchical clustering based on LOH patterns distinguished major molecular subsets of HGSC, which were remarkably consistent in all 3 data sets. HGSC were similar to TNBC in their degree of LOH and distinct from HER2-positive and ER-positive high-grade cancers. Subtypes of HGSC defined by

profiles of LOH differed in their sensitivity to first-line platinum- and taxane-based chemotherapy. Quartiles of LOH burden correlated with progression-free survival (PFS) after surgery and chemotherapy, even in patients without mutations in *BRCA1* or *BRCA2*.

Materials and Methods

Subjects and tissues from Boston

Ovarian cancer tissue was collected at the Dana-Farber Cancer Institute and Brigham and Women's Hospital (Boston, MA) along with treatment and outcome information. All tumors were serous, grade 2 or 3; grade 1 tumors were excluded. Forty-seven cases passed quality control and were analyzed (Supplementary Table S1). Fifty Bloom-Richardson grade 3 breast cancer cases were from a larger study of breast cancer, described elsewhere (21). All tissue samples and clinical information were identified and collected under a Dana-Farber/Harvard Cancer Center Institutional Review Board-approved protocol.

HGSC were considered platinum resistant if there was progressive disease during initial chemotherapy or evidence of progression within 6 months after completion of chemotherapy, and platinum sensitive if disease did not recur or progress within 6 months after completion of initial chemotherapy (15, 22, 23). All patients underwent debulking surgery before platinum- and taxane-based chemotherapy. Optimal debulking resulted in 1 cm or less of residual tumor and suboptimal debulking left more than 1 cm; 23 patients had optimal debulking surgery. Most cases (73%) were stage III, 18% stage IV, and 9% stage II (Supplementary Table S1).

Enrichment of tumor cells and DNA preparation

Ovarian and breast tumor cells were enriched by needle microdissection to remove stromal components from 7 μ m frozen sections lightly stained with hematoxylin and eosin. Tumor cells were isolated from ascites by affinity enrichment with anti-EPCAM-conjugated beads as described (24). The preparation of DNA and RNA was described previously (6).

SNP and gene expression array analysis

Genomic DNA digested with NspI was hybridized to Affymetrix GeneChip Human Mapping 250K NspI arrays using recommended procedures (Affymetrix, Inc.). The data have been submitted to and will be posted in GEO (GSE39130). 10K SNP data from 50 breast cancers have been described (ref. 21; GSE19594). LOH was determined by comparing genotype calls (heterozygous or homozygous) from tumor and matched normal cells in blood or morphologically normal breast tissues. For tumors without a paired normal sample from the same patient, LOH was defined by an LOH prediction algorithm in dChip software (25, 26). We compared patterns and overall frequency of LOH derived from 10K and 250K SNP arrays and the results were similar (Supplementary Fig. S1).

LOH-based hierarchical clustering was done based on significant LOH patterns using algorithms running on

dChip software as described (27). Significantly frequent LOH regions were identified by a permutation test carried out across the entire cohort (permutation $P < 0.05$). These significant regions were used for hierarchical clustering. The distance between any 2 individuals was defined as the proportion of discordance among significantly frequent LOH regions. The average-linkage algorithm is divisive and merges samples into clusters, based on similarity of LOH patterns (27). Differences between 2 adjacent specimens are represented by the length of the vertical lines in the clustering dendrogram.

To estimate and minimize the effect of stromal contamination, we used major copy proportion (MCP) analysis to measure AI, an alternative allele copy ratio-based approach for LOH analysis (28). MCP is the ratio of the copy number of the major allele divided by the copy number for both major and minor alleles. The MCP scores for heterozygous and homozygous loci are 0.5 and 1.0, respectively. In a homogeneous tumor sample, an MCP score of 1.0 at a heterozygous locus represents AI with complete allelic loss of one parental copy (LOH). MCP scores will shift down from 1.0 when normal heterozygous alleles contaminate the tumor samples (28). More than 20% contamination shifts MCP scores to less than 0.7 in regions of AI that possess an absolute copy number decrease. Such samples were excluded. Samples containing regions of AI with absolute copy number decrease and MCP scores of 0.7 or more were considered acceptable and included in this study. Scoring and mapping of LOH and MCP, and DNA copy number analysis were conducted using dChip.

Affymetrix Human Genome U133 Plus 2.0 arrays were used to analyze gene expression in 25 cases in which RNA was available. Expression data were normalized using a model-based algorithm in dChip software.

BRCA1 methylation assay

DNA was treated with bisulfate using EZ DNA Methylation-Direct (ZYMO Research, Inc.) after protocols from the manufacturer. Tests for *BRCA1* promoter methylation were conducted by methylation-specific PCR with modifications as described previously (29, 30).

AOCS and TCGA ovarian cancer cohorts

Datasets from the AOCS were obtained using Affymetrix Human Mapping 50K Xba 240 SNP arrays and were downloaded from GEO, NCBI accession number GSE13813. Treatment and outcome information from the initial report was updated for this study (23). Samples in the AOCS cohort were needle microdissected to remove stromal cells. Optimal debulking was achieved in 50 patients, 25 patients had a suboptimal debulking, and data were incomplete in 10 patients (Supplementary Table S2). AOCS data for *BRCA1* and *BRCA2* germline mutations were available for a subset of patients included in this manuscript, and are described in more detail (31). These AOCS samples were collected as part of a study that was approved by the Human Research Ethics Committees at the Peter MacCallum Cancer

Centre, Queensland Institute of Medical Research, and all other participating hospitals.

A comprehensive genomic dataset of HGSC was released by TCGA (32). Affymetrix Genome-Wide Human SNP Array 6.0 was used by TCGA. Entry criteria included a content of nontumor nuclei 20% or less (80% tumor content); microdissection was not mandated in TCGA. One hundred sixteen patients chosen from the TCGA were stage III, tumors were grade 3, and all patients underwent optimal debulking surgery. Of these patients, information on both germline and somatic *BRCA1* and *BRCA2* gene mutations was available for 78 patients. Follow-up for 12 of them was incomplete. Information about TCGA patients included in this study can be found in Supplementary Table S3.

Statistical analysis

The fraction of each tumor genome with LOH (FLOH) was calculated as the proportion of inferred LOH calls within the total number of SNPs. The number of chromosomal regions with AI was enumerated across each tumor genome. We used dChip software to score the prevalence of LOH, and permuted these results to define genome-wide peaks of LOH unlikely to be random ($P < 0.05$).

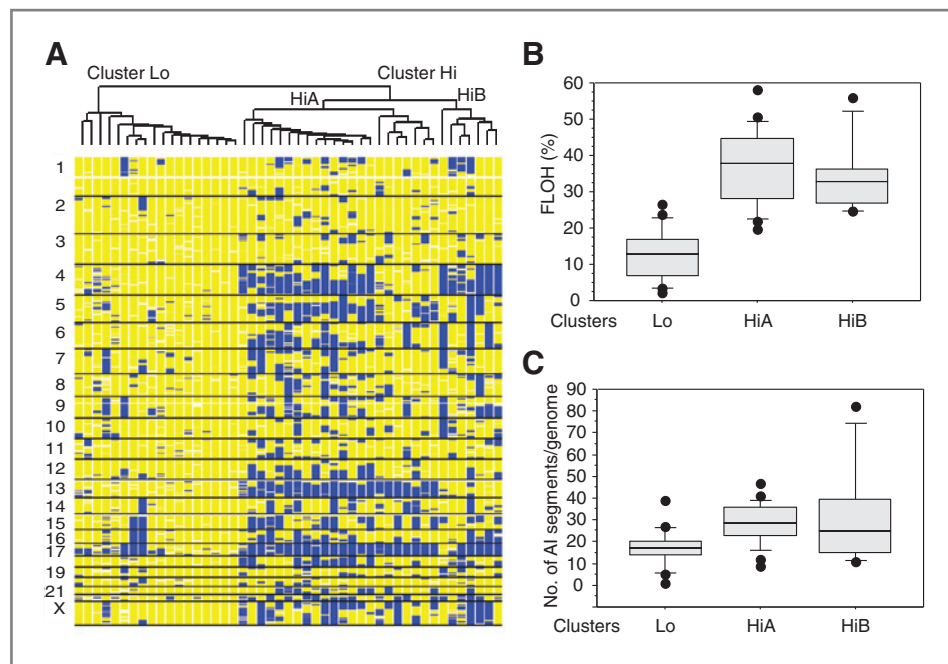
Statistical significance was evaluated by nonparametric analysis using the Mann-Whitney U test for comparisons of 2 groups and the Kruskal-Wallis H test for comparisons between 3 and more groups. Pearson correlation was used to find the correlation coefficient between FLOH levels and resistance rates, and χ^2 was used to evaluate the difference among groups of HGSC. Logistic regression was used for multivariate analysis. Kaplan-Meier analysis was used to evaluate clinical outcome after chemotherapy. The difference between Kaplan-Meier curves was evaluated by the log-rank test.

Results

Genomic profiling HGSCs of ovary

We conducted genome-wide LOH analysis in 47 HGSC specimens from Boston. Heterogeneity of LOH patterns in HGSC was observed, and 2 top clusters were identified and separated using LOH-based hierarchical clustering as described in Materials and Methods (Fig. 1A). A major cluster of 29 cases (62%) harbored massive intra- and whole-chromosomal LOH across each tumor genome (cluster Hi; Fig. 1A). This major cluster harbored a mean FLOH of 36.3% and contrasted with a minor cluster with a low frequency of LOH events (cluster Lo, mean FLOH = 12.8%; Fig. 1A and B). Hierarchical clustering further separated the major cluster Hi into 2 subclusters (HiA and HiB; Fig. 1A). The subclusters of the Hi cluster showed similar levels of LOH (mean FLOH = 37.9% and 32.7%; Fig. 1B), but differed in the regions of LOH involved. Loss or near loss of 1 parental copy of the acrocentric chromosome 13 was seen almost exclusively in subcluster HiA, and LOH of 5q and 17p was more frequent in subcluster HiA (Fig. 1A and Supplementary Table S4).

Figure 1. LOH-based hierarchical clustering of HGSC. **A**, LOH-based clustering of 47 ovarian cancers. The clustering dendrogram is depicted at the top, and each column represents the genome-wide status of heterozygosity; yellow, region of retained heterozygosity; blue, region of LOH. Chromosome location is indicated on the vertical axis. **B**, box plots depicting fraction of LOH (FLOH) for HGSC in cluster Lo and cluster HiA and HiB from **A**. The horizontal line within the box is the median value of FLOH. **C**, box plots showing number of chromosomal segments containing allelic imbalance (AI) per cancer genome.



Nonmalignant cells could interfere with proper genotype calls from tumor-derived DNA. All cases were microdissected and the proportion of tumor cells to normal cells was estimated to equal or exceed 90%. To minimize the influence of normal contamination that could contribute to the appearance of cluster Lo, with low FLOH, we calculated AI using major copy proportion (MCP; ref. 28). The number of genomic regions with AI were significantly lower in cluster Lo, and the overall pattern was consistent with the presence of distinctive groups of HGSC defined by LOH profiles (Fig. 1C and Supplementary Fig. S2).

We compared the genomic patterns of HGSC with high-grade breast cancers by conducting LOH-based clustering in a group of 50 breast tumors. These cancers contained 15 high-grade ER-positive, 10 HER2-positive, 20 sporadic TNBC, and 5 additional cases from women with inherited *BRCA1* mutations. One major cluster was dominated by TNBC and *BRCA1*-associated tumors. A second cluster was dominated by HER2-positive and high-grade ER-positive cancers (Supplementary Fig. S3A). Sporadic TNBC and *BRCA1*-associated breast cancers possessed a significantly higher median FLOH ($P < 0.0001$) and number of AI regions per genome ($P < 0.0002$) compared with HER2-positive and high-grade ER-positive tumors (Supplementary Fig. S3B and S3C). Therefore, HGSC and TNBC share high levels of LOH.

LOH patterns and copy number alterations

We examined qualitative patterns of LOH and copy number gains and losses in LOH-defined clusters of HGSC. In HGSC-Hi, regions of common LOH reached a prevalence of $\geq 50\%$ in 15 chromosomes. Uniparental loss of the entire, or nearly the entire chromosome 17 was seen in all but one case of HGSC-Hi and less common in HGSC-Lo.

Permutation testing defined a threshold level of significance ($P \leq 0.05$) for LOH regions on chromosomes 4q, 5q, 6q, 13q, 17p, and 17q in HGSC-Hi (Fig. 2A). Similar to allelic loss, copy number loss was a prominent feature of HGSC-Hi, and less common in HGSC-Lo (Fig. 2B). In contrast to the allelic and copy loss, copy gains were common and remarkably similar in both cluster Hi and cluster Lo of HGSC (Fig. 2B). Allelic loss may be either an absolute loss of DNA content, or copy neutral loss of a parental allele. In HGSC-Hi, allelic loss was approximately equally divided between hemizygosity and isodysomy. Loss, particularly allelic loss, seems to define subclusters of HGSC.

In TNBC, regions of common LOH reached a prevalence of 50% on 15 chromosomes; however, permutation testing with a threshold of $P \leq 0.05$ revealed significant LOH on chromosomes 5q, 11q, 14q, 17p, and 17q. In high-grade ER-positive and HER2-positive breast cancer, significant regions of LOH were seen only on chromosomes 8p and 17p, and patterns were different than observed in TNBC. When comparing HGSC-Hi to TNBC, with the exception of chromosome 17 and 5q, patterns of significant LOH regions were quite different (compare Fig. 2A to Supplementary Fig. S4). Copy number gains were commonly seen in TNBC and high-grade luminal breast cancers (ER-positive and HER2-positive; Supplementary Fig. S4).

BRCA1 promoter methylation

BRCA1 methylation was detected in 9 of 44 HGSC (20%) and 3 of 18 sporadic TNBC tumors (17%). More tumors in HGSC-Hi than HGSC-Lo possessed methylated *BRCA1* promoter regions (30.7% vs. 5.5%, respectively, $P < 0.042$; Fig. 3A). FLOH was higher and *BRCA1* transcript levels were lower in HGSC tumors with *BRCA1* promoter methylation than in those without this event ($P < 0.019$ and

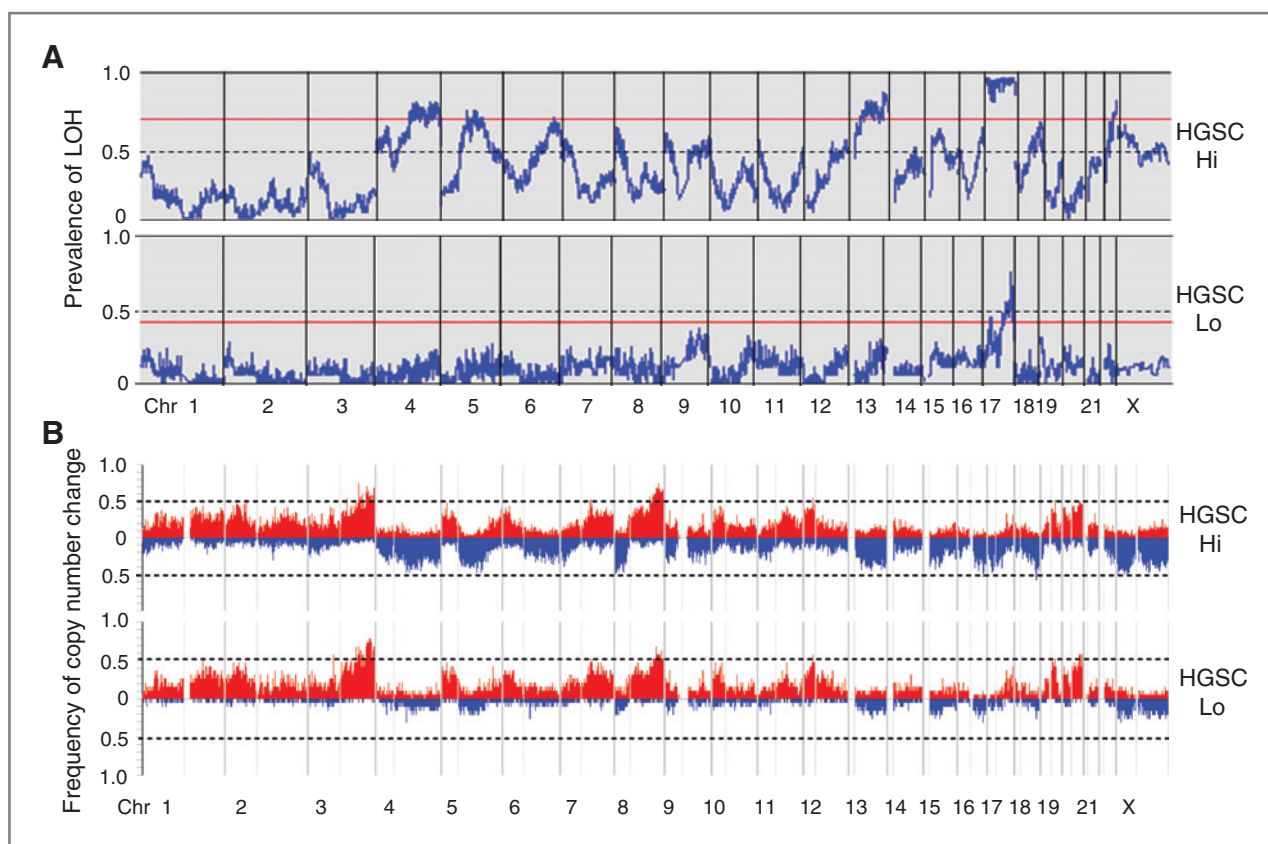


Figure 2. Genome-wide prevalence of LOH in HGSC. Chromosome location is on the horizontal axis. Horizontal red lines represent a threshold P value ≤ 0.05 by genome-wide permutation. A, genome-wide prevalence of LOH. B, frequency of genome-wide copy number gain and loss. Frequency of absolute copy gain ≥ 3 (red) and copy loss ≤ 1.4 (blue) for each SNP is shown on the vertical axis. The light vertical lines separate the short and long arms.

$P < 0.053$, respectively; Fig. 3B and C). These results are consistent with the notion that *BRCA1* promoter methylation suppresses *BRCA1* expression and contributes to chromosomal instability.

Validation of LOH-based clustering in independent datasets of HGSC

LOH-based hierarchical clustering of ovarian cancer was validated using datasets from the AOCs and TCGA. Normal stromal cells in tumors from the AOCs were removed by needle microdissection, as was done with the Boston cases. The TCGA required tumors have at least 80% tumor cells in blocks used for analysis. Hierarchical clustering based on LOH separated 85 cases from the AOCs into 2 clusters: a minor subset (Cluster Lo) of 18 tumors with relatively lower LOH levels (mean FLOH = 5.1%) and a major cluster (Cluster Hi) with 67 tumors (Fig. 4A). As observed in the Boston dataset, cluster Hi could be divided into 2 subclusters (HiA and HiB), which had mean FLOH levels of 31.5% and 21.6%, respectively.

Clustering 116 HGSC in the TCGA produced a similar topology of subclusters (Fig. 4B). Again, subcluster HiA was associated with loss of chromosome 13q, whereas subcluster HiB retained both parental copies of 13q in both the AOCs and TCGA samples (Fig. 4A–B and Supplementary

Table S4). Loss of one parental copy of chromosome 17 was a striking feature of tumors in Cluster Hi from both the AOCs and TCGA, and was less common in Cluster Lo tumors. The 3 major clusters (Cluster Lo, and subclusters HiA and HiB) were remarkably reproducible in all 3 cohorts studied.

Tohill and colleagues described 4 gene expression-based molecular subtypes of HGCS (4). These subtypes were reproduced in data from the TCGA (data not shown). We found a trend toward the association of cases in molecular subtype C1 with our LOH-based cluster HGSC-Lo in the AOCs cohort ($P = 0.063$), but not in the TCGA (data not shown).

LOH and impact on treatment resistance

To explore the relationship between the LOH-defined subclusters of HGSC and clinical outcome, we compared chemotherapy-resistant rates for patients pooled from all 3 cohorts. The frequency of platinum-resistant disease (progression or recurrence within 6 months after completion of primary platinum-based chemotherapy) was different for each subcluster (Lo, HiA, and HiB). In patients with stage III disease and optimal debulking, the HiA subcluster, which had the highest FLOH, had the lowest resistance rate compared with the 2 other subclusters (Fig. 5A and B and

Supplementary Table S5A). The Lo cluster, which harbored tumors with the lowest FLOH, had the highest chemotherapy-resistance rates. These trends generally remained same when data from all patients irrespective of stage and debulking status were analyzed (Fig. 5C and D and Supplementary Table S5B). When the 3 cohorts were analyzed individually, HiA had the lowest resistance rates and cluster Lo had the highest rates of chemotherapy resistance (Supplementary Fig. S5A and S5B). Resistance rates were inversely correlated to the mean FLOH of subclusters when the results from the 3 cohorts were plotted together (Pearson correlation, coefficient = -0.6 , $P < 0.041$; Supplementary Fig. S5C).

Because at least 20% of HGSC harbor either germline or somatic mutations in *BRCA1/2* (3, 33), we questioned whether *BRCA1* and *BRCA2* germline mutations account for the better initial response to chemotherapy in patients within the HiA group. Data were available for a subset of 39 AOCs patients, including 10 with either *BRCA1* or *BRCA2* germline mutations. Tumors from *BRCA1/2* mutation carriers were concentrated in subclusters HiA and HiB (Supplementary Table S6). Tumors from mutation carriers had a significantly higher FLOH than tumors in HGSC-Lo and HiB from noncarriers, but were similar to tumors from noncarriers in subcluster HiA (Supplementary Fig. S6A). After removing the mutation carriers, the patients with tumors in the HiA subcluster still had low rates of chemotherapy resistance (Supplementary Fig. S6B). The same was true for the HiA subcluster when we combined AOCs and TCGA patients (Supplementary Fig. S6C). In the combined data, there was a tendency for tumors with *BRCA* mutations to have a lower resistance rate to initial chemotherapy, but this tendency did not reach statistical significance. HiA was further tested against other covariates, including *BRCA* gene status and FLOH, in a multivariate analysis with platinum resistance as the outcome using data from the AOCs and TCGA (Supplementary Table S7). Belonging to cluster HiA was the only significant predictor of being platinum sensitive in patients after successful debulking surgery.

LOH and impact on outcome

We examined PFS in LOH-defined subclusters in the 3 cohorts. Patients in the HiA subcluster had a longer median PFS compared with the other 2 subclusters in all 3 cohorts, even after removing *BRCA1/2* mutation carriers from the AOCs and TCGA datasets, although the differences were not statistically significant (Supplementary Table S8).

We evaluated LOH burden in tumors, irrespective of the subclusters and clinical outcome for patients with stage III HGSC and residual disease of 1 cm or less in the Boston and AOCs cohorts. Patients were separated by quartiles of FLOH in their tumors. HGSC patients in the fourth quartile with the highest FLOH had longer PFS; however, the relationships were nonmonotonic. Except for patients with early disease progression, patients in the first quartile with the lowest FLOH also enjoyed a longer PFS; whereas patients whose tumors were in the second quartile with intermediate FLOH had the shortest PFS (Fig. 6A and B). Similar trends were seen when the cases with stage II and IV disease and

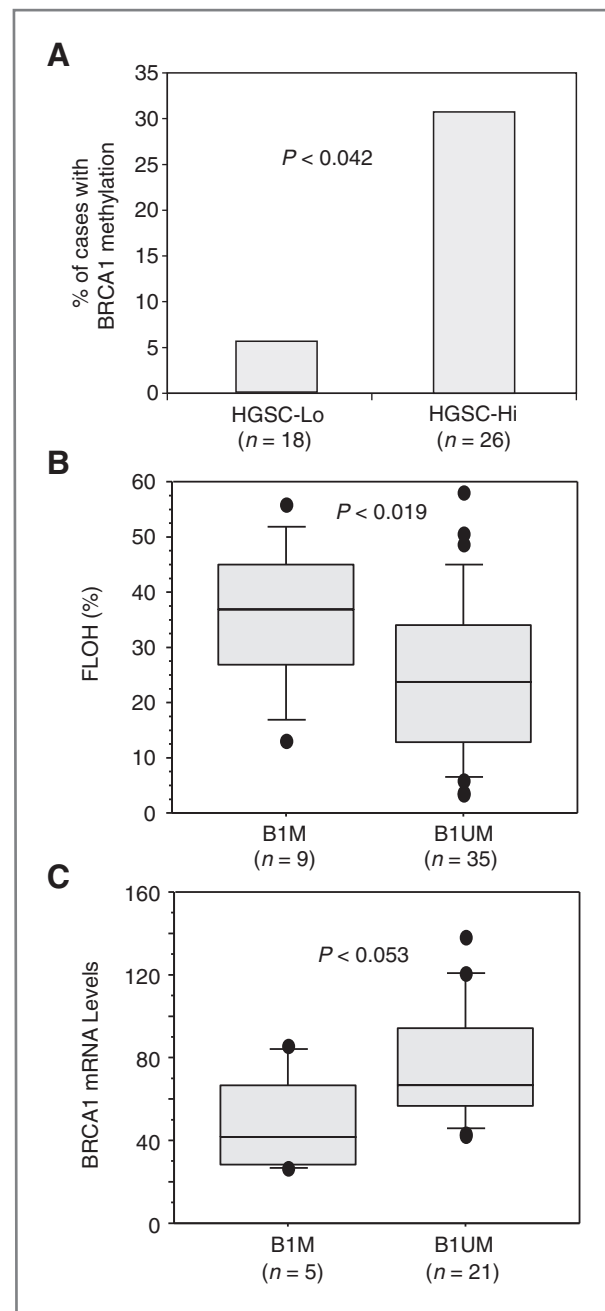


Figure 3. *BRCA1* promoter methylation, FLOH and *BRCA1* transcript levels in HGSC. A, frequency of *BRCA1* promoter methylation in HGSC. P value was obtained by using 2-way contingency analysis and Chi square. B, *BRCA1* promoter methylation and FLOH in HGSC. FLOH was compared between cases with *BRCA1* promoter methylation (B1M) and cases without *BRCA1* methylation (B1UM). C, *BRCA1* promoter methylation and *BRCA1* mRNA levels. P value is determined by Mann-Whitney U tests.

suboptimal debulking were included (Supplementary Fig. S7A and S7B). The relationship between FLOH quartiles and PFS was not clearly seen in TCGA, which may be due to interinstitutional variation in PFS across TCGA. After removing *BRCA1/2*-mutation carriers from the AOCs

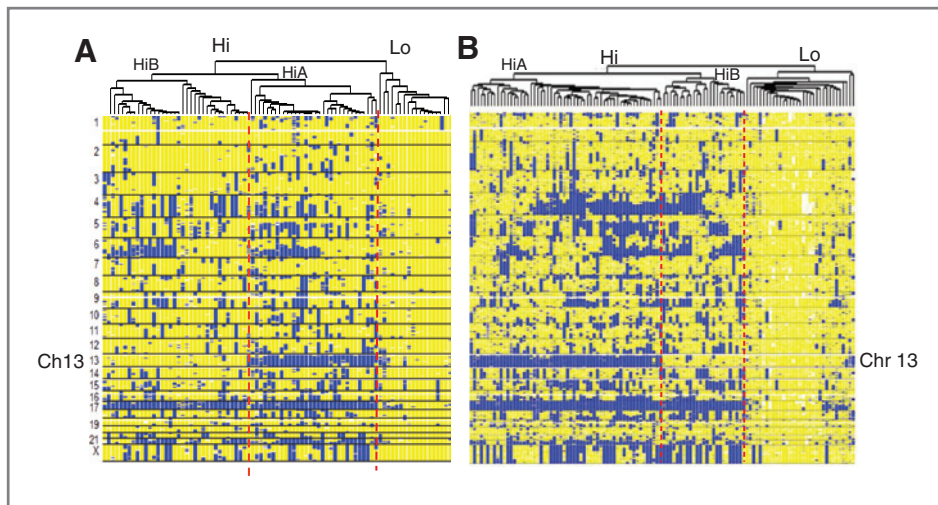


Figure 4. Genomic profiles of HGSC in AOCs and TCGA SNP array datasets. A, hierarchical clustering and visualization based on LOH patterns in the AOCs dataset. B, hierarchical clustering in the TCGA dataset.

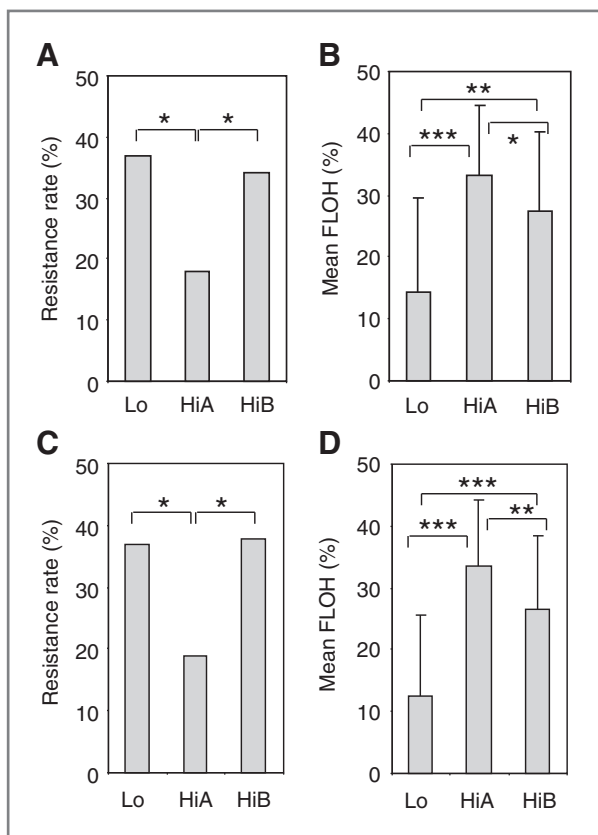


Figure 5. FLOH and rate of resistance to platinum-based chemotherapy in subclusters of HGSC from three independent cohorts. A and B, chemotherapy resistance and mean FLOH in tumors from subclusters Lo, HiA, and HiB for patients with stage III disease and residual disease ≤ 1 cm after optimal debulking, pooled from the 3 cohorts. C and D, results from all patients including those with stages II and IV cancer and residual disease > 1 cm. *P* values are derived from Chi square analysis using 2-way contingency tables in A and C, and from *t* test in B and D. *, **, and *** represent *P* values < 0.05 , < 0.001 , and < 0.00001 , respectively.

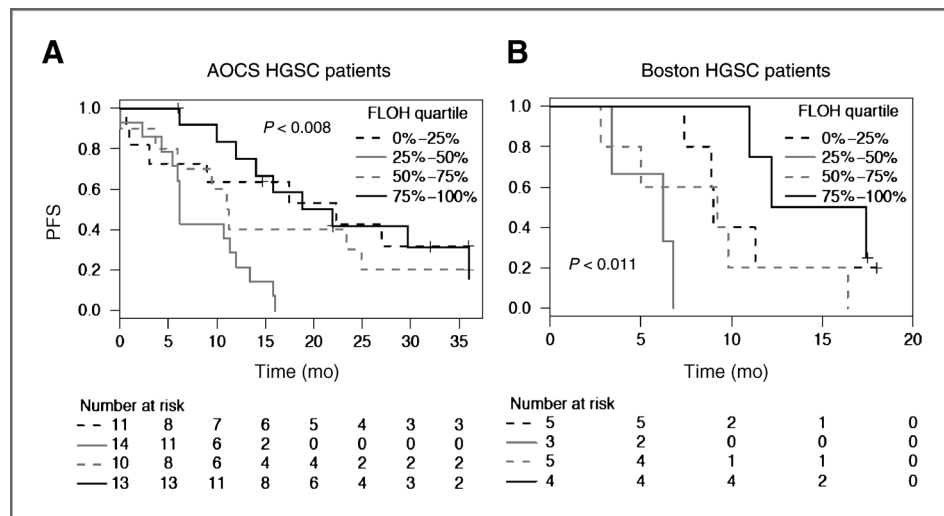
dataset, the same nonmonotonic relationship between tumor FLOH and patient's PFS remained (Supplementary Fig. S8). The PFS for *BRCA1/2* mutation carriers was similar to noncarriers with tumors in the highest FLOH quartile. Ovarian cancer with germline *BRCA1/2* mutations have a higher mean FLOH level, and are known to be platinum sensitive. In this analysis, evidence emerges that high FLOH without *BRCA1/2* mutation may also mark tumors more sensitive to platinum-based chemotherapy and with better outcomes.

Discussion

HGSC is the most common subtype of epithelial ovarian cancer and has distinct molecular features, including p53 mutations, genetic instability, and mutations in *BRCA1* or *BRCA2* (1–3, 11). This study identified remarkable genomic heterogeneity in HGSC otherwise considered histologically homogeneous. Two dominant groups of HGSC were uncovered by hierarchical clustering based on common regions of LOH; the major group possessed high-level LOH/AI (HGSC-Hi) and the minor group had lower levels of LOH/AI (HGSC-Lo). HGSC-Hi was further separated into 2 subclusters (HiA and HiB) based on specific regions of chromosomal loss. The HiA, HiB, and Lo pattern was nearly identical in 3 independent studies of HGSC (Figs. 1A and 4).

To compare ovarian and breast cancer, we selected a cohort of exclusively high-grade breast cancers containing HER2-positive, high-grade ER-positive, and TNBC. HGSC-Hi and TNBC harbor similar amounts of copy loss and allelic loss, and more than seen in HGSC-Lo and in other breast cancer subtypes. These findings imply shared mechanism(s) of failed DNA repair have a similar overall impact on HGSC and TNBC genomes. However, cell lineage-specific factors may select for specific regions of LOH in the 2 different cancers. The concept of "BRCAness" has been advanced to describe the phenotypic and molecular relatedness of certain breast and ovarian cancers to tumors without germline inactivation of *BRCA1* and *BRCA2*

Figure 6. Progression-free survival (PFS) after surgery and chemotherapy. Kaplan–Meier analysis was done in patients with stage III disease and 1 cm or less residual cancer after surgery; all patients received platinum and taxane combination chemotherapy. A, the AOCs cohort; B, the Boston cohort. Patients were divided into quartiles of FLOH (from low to high) in their tumors. *P* values are calculated by log-rank test. Patients who were progression-free at the time of last follow-up were censored (+).



(34, 35). Past or ongoing failure of DNA repair may contribute to chromosomal instability and the pathogenesis of sporadic TNBC and HGSC-Hi, and the repair defect may be functionally equivalent to the failure of *BRCA1* or *BRCA2* in hereditary ovarian and breast cancers (19, 20, 36).

In addition to germline and somatic mutations in *BRCA1* and *BRCA2*, methylation of other members of the pathway has been reported, including epigenetic modification of the *BRCA1* promoter (3, 33). In both the Boston and TCGA cohorts, there was a correlation between *BRCA1* promoter methylation and decreased *BRCA1* expression. In the Boston cohort, methylated *BRCA1* promoter was associated with high FLOH; however, this relation was not significant in TCGA (data not shown). There was a trend toward low *BRCA1* transcripts and high FLOH in tumors without *BRCA1* mutations in TCGA, but this relationship was not significant (Supplementary Fig. S9). In the cases without *BRCA1* mutations, defects in other DNA repair-associated genes may contribute to genomic instability marked by high FLOH. TCGA compared clinical outcome with different mechanisms of *BRCA1* inactivation. Although patients with somatic or germline mutations in *BRCA1* had improved responses to chemotherapy and overall survival, patients with methylation of the *BRCA1* promoter had similar survival characteristics to patients without obvious defects in the *BRCA* pathway (3). Tumor genomes are complex and methylation of the *BRCA1* promoter may be part of global methylation that effects the expression of multiple genes and will have a complex impact on the tumor genome and treatment outcome.

Intrinsic defects in HR in sporadic HGSC and TNBC may force the execution of "error prone" pathways that repair double-strand DNA breaks, otherwise more faithfully repaired by HR. One of these error prone pathways is nonhomologous end joining (NHEJ). Stephens and colleagues sequenced both ends of randomly generated DNA fragments in breast cancer cell lines and tissue to detect somatic genetic recombination (37). Recombination was common in breast cancer, particularly within TNBC, and

from tumors or cell lines containing germline *BRCA1* mutations. Recombination was recognized by discordant sequences on either end of the DNA fragment spanning the breakpoint. The fusion junction commonly contained regions of microhomology and small insertions of non-templated DNA. These features are considered "signatures" of NHEJ and frequent in *BRCA1*-associated and TNBC (37, 38). A high burden of LOH within a tumor is a hallmark for this type of chromosomal aberration. Tumors in the HGSC-Hi cluster bear this hallmark of defective HR and these cancers may be forced into NHEJ and accumulate allelic loss.

HGSC-Lo, with a lower burden of LOH, may represent a distinct subset of HGSC with apparently intact DNA repair capability. Recent studies involving *ex vivo* DNA damage of tumor samples has shown that about one third of HGSC retain the ability to form RAD51 foci and therefore seem to have intact HR pathways (39). HGSC-Lo may represent those tumors with intact HR pathways, perhaps evolved from low-grade serous tumors carrying *RAS*, *PI3K*, or *BRAF* mutations (1, 2, 40), or the result of variants in which defects in HR are partially corrected or compensated for during tumor progression (41). Impaired HR may also sensitize HGSC to repair pathways that depend on the multifunctional enzyme poly (ADP-ribose) polymerase 1 (PARP1) (42, 43). Clinically, HGSC-Lo is a subgroup of ovarian cancer that may not be sensitive to PARP1 inhibitors, whereas the cancers in subcluster HiA may be more sensitive.

Membership in HiA was the only predictor of platinum-sensitivity surviving multivariate analysis that included *BRCA* status and FLOH. In addition, excluding *BRCA* mutation carriers and somatic *BRCA* mutations from analysis, tumors in subcluster HiA remain the most sensitive to platinum treatment. Allelic loss of chromosome 13 is a signature of membership in HiA. Expression of critical genes may be lost or reduced as a result losing one parental copy of chromosome 13. The endosome copper-transporters *ATP7A* and *ATP7B* are the 2 major proteins that pump

platinum out of cells and away from the nucleus (44). Genes for ATP7B and ATP7A are located on chromosomes 13 and X, respectively. Growing evidence suggests increased expression of ATP7B is particularly associated with platinum resistance in ovarian cancer (45). A nuclear excision repair gene *ERCC5* on 13q33.1, critical for removing platinum-caused DNA adducts, is a prognostic biomarker in ovarian cancer (46). Both *RB1* and *BRCA2* are located on 13q, and may be affected by allelic loss of a parental copy of chromosome 13. It is possible that genes on chromosome 13q contribute to chemotherapy sensitivity in ovarian cancer, in addition to the burden of LOH and impaired DNA repair. Sensitivity to genotoxic chemotherapy is predicted by HiA class membership; however, outcomes such as PFS may depend on other factors, and may be more complicated.

This study found a nonmonotonic relationship between content of LOH and PFS, with shorter PFS in tumors with an intermediate content of LOH (Fig. 6 and Supplementary Fig. S6). A similar "J-shaped" nonmonotonic relationship was described between recurrence-free survival and quartiles of a gene expression signature reflecting chromosomal instability (CIN70) in 13 publically available cohorts of chemotherapy-treated patients. In that report, highest and intermediate CIN70 signatures were associated with the longest and shortest recurrence-free survival after adjuvant multidrug chemotherapy, respectively, in multiple cancer types including TNBC and ovarian cancer (47). We observed a paradoxical longer PFS for patients whose tumors contained the lowest quartile of FLOH, except for those having an early disease progression. This result may reflect the more indolent biology of tumors with a low burden of LOH, or in part because of the effects of taxanes used in combination with platinum.

Evidence suggests relative resistance to taxanes in breast and ovarian cancers with *BRCA1* deficiency (48). Ovarian cancers with the higher CIN70 signatures were more taxane resistant in a clinical trial of taxane monotherapy (49). In metastatic breast cancer, taxane monotherapy was less effective in carriers of *BRCA1* mutations compared with patients without mutations in this gene (50). It is possible that HGSC with less LOH, a lower CIN70 signature and more stable genomes may be more sensitive to taxanes. Increased sensitivity to taxanes may explain the longer PFS in our patients whose ovarian cancers harbored the lowest quartile of LOH. Patients with tumors that are *BRCA1/2* mutation associated or those in HGSC-HiA (with the highest levels of LOH), may benefit by genotoxic chemotherapy, alone or with newer agents such as PARP inhibitors that target DNA repair.

References

1. Kurman RJ, Shih Ie M. Pathogenesis of ovarian cancer: lessons from morphology and molecular biology and their clinical implications. *Int J Gynecol Pathol* 2008;27:151-60.
2. Bowtell DD. The genesis and evolution of high-grade serous ovarian cancer. *Nat Rev Cancer* 2010;10:803-8.
3. Bell D, Berchuck A, Birrer M, Chien J, Cramer DW, Dao F, et al. Integrated genomic analyses of ovarian carcinoma. *Nature* 2011;474:609-15.
4. Tothill RW, Tinker AV, George J, Brown R, Fox SB, Lade S, et al. Novel molecular subtypes of serous and endometrioid ovarian cancer linked to clinical outcome. *Clin Cancer Res* 2008;14:5198-208.
5. Helland A, Anglesio MS, George J, Cowin PA, Johnstone CN, House CM, et al. Deregulation of MYCN, LIN28B and LET7 in a molecular subtype of aggressive high-grade serous ovarian cancers. *PLoS One* 2011;6:e18064.

Disclosure of Potential Conflicts of Interest

No potential conflicts of interest were disclosed.

Authors' Contributions

Conception and design: Z.C. Wang, J. Quackenbush, J.D. Iglehart, U.A. Matulonis

Development of methodology: Z.C. Wang, A. Culhane, J. Quackenbush, U.A. Matulonis

Analysis and interpretation of data (e.g., statistical analysis, bio-statistics, computational analysis): Z.C. Wang, N.J. Birkbak, A. Culhane, M. Schwede, K. Alsop, A. Miron, H.B. Salvesen, J. Quackenbush, J.D. Iglehart, D.D. Bowtell, U.A. Matulonis

Acquisition of data (provided animals, acquired and managed patients, provided facilities, etc.): R.I. Drapkin, A. Fatima, R. Tian, K.E. Daniels, J. Liu, D. Etemadmoghadam, A. Miron, H.B. Salvesen, G. Mitchell, A. DeFazio, R.S. Berkowitz, D.D. Bowtell, U.A. Matulonis

Writing, review, and/or revision of the manuscript: Z.C. Wang, A. Culhane, R.I. Drapkin, M. Schwede, K. Alsop, D. Etemadmoghadam, H.B. Salvesen, G. Mitchell, A. DeFazio, J. Quackenbush, R.S. Berkowitz, J.D. Iglehart, D.D. Bowtell, U.A. Matulonis

Administrative, technical, or material support (i.e., reporting or organizing data, constructing databases): K.E. Daniels, H. Piao, J. Liu, H.B. Salvesen, J. Quackenbush, U.A. Matulonis

Study supervision: J.D. Iglehart, U.A. Matulonis

Making certain that all patient specimens and clinical data collection was conducted in an IRB-approved manner: U.A. Matulonis

Acknowledgments

The authors thank Christopher Crum and Michele Hirsch for ovarian cancer tissue bank support and for histologically grading the Boston cohort of tumors, Emily Kantoff for assistance in clinical data collection, and the Dana-Farber microarray core for generation of SNP array data. We are indebted to Dr Cheng Li at Dana-Farber for modifying the dChip software program to conduct clustering analyses.

Grant Support

This study was funded by the Breast Cancer Research Foundation, New York, NY. Funds from the Susan F. Smith Center for Women's Cancers Program at Dana-Farber Cancer Institute partially supported the genomic studies. N. J. Birkbak was funded by the Danish Council for Independent Research-Medical Sciences (FSS). R. Drapkin was supported by Ovarian Cancer SPORE P50 CA105009, Ovarian Cancer Research Fund, and Robert and Deborah First Fund. The Australian Ovarian Cancer Study was supported by the U.S. Army Medical Research and Materiel Command (DAMD17-01-1-0729), the US Department of Defense (W81XWH-08-1-0684 and W81XWH-08-1-0685), Cancer Australia and National Breast Cancer Foundation (509303), the Peter MacCallum Cancer Centre Foundation, Cancer Council Victoria, Queensland Cancer Fund, Cancer Council New South Wales, Cancer Council South Australia, Cancer Foundation of Western Australia, Cancer Council Tasmania, and the National Health and Medical Research Council of Australia (NHMRC). The Gynaecological Oncology Biobank at Westmead, a member of the Australasian Biospecimen Network-Oncology group, is also funded by NHMRC. H. B. Salvesen was supported by funds from The Norwegian Cancer Society and The Research Council of Norway.

The costs of publication of this article were defrayed in part by the payment of page charges. This article must therefore be hereby marked *advertisement* in accordance with 18 U.S.C. Section 1734 solely to indicate this fact.

Received March 20, 2012; revised July 25, 2012; accepted August 13, 2012; published OnlineFirst August 21, 2012.

6. Wang ZC, Lin M, Wei LJ, Li C, Miron A, Lodeiro G, et al. Loss of heterozygosity and its correlation with expression profiles in subclasses of invasive breast cancers. *Cancer Res* 2004;64:64-71.
7. Richardson AL, Wang ZC, De Nicolo A, Lu X, Brown M, Miron A, et al. X chromosomal abnormalities in basal-like human breast cancer. *Cancer Cell* 2006;9:121-32.
8. Perou CM, Sorlie T, Eisen MB, van de Rijn M, Jeffrey SS, Rees CA, et al. Molecular portraits of human breast tumours. *Nature* 2000;406:747-52.
9. Sorlie T, Tibshirani R, Parker J, Hastie T, Marron JS, Nobel A, et al. Repeated observation of breast tumor subtypes in independent gene expression data sets. *Proc Natl Acad Sci U S A* 2003;100:8418-23.
10. Lim E, Vaillant F, Wu D, Forrest NC, Pal B, Hart AH, et al. Aberrant luminal progenitors as the candidate target population for basal tumor development in BRCA1 mutation carriers. *Nat Med* 2009;15:907-13.
11. Ahmed AA, Etemadmoghadam D, Temple J, Lynch AG, Riad M, Sharma R, et al. Driver mutations in TP53 are ubiquitous in high grade serous carcinoma of the ovary. *J Pathol* 2010;221:49-56.
12. Futreal PA, Liu Q, Shattuck-Eidens D, Cochran C, Harshman K, Tavtigian S, et al. BRCA1 mutations in primary breast and ovarian carcinomas. *Science* 1994;266:120-2.
13. Foulkes WD, Stefansson IM, Chappuis PO, Begin LR, Goffin JR, Wong N, et al. Germline BRCA1 mutations and a basal epithelial phenotype in breast cancer. *J Natl Cancer Inst* 2003;95:1482-5.
14. Muggia F. Platinum compounds 30 years after the introduction of cisplatin: implications for the treatment of ovarian cancer. *Gynecol Oncol* 2009;112:275-81.
15. Liu J, Matulonis U. Rational use of cytotoxic chemotherapy for recurrent ovarian cancer. *J Natl Compr Canc Netw* 2006;4:947-53.
16. Silver DP, Richardson AL, Eklund AC, Wang ZC, Szallasi Z, Li Q, et al. Efficacy of neoadjuvant Cisplatin in triple-negative breast cancer. *J Clin Oncol* 2010;28:1145-53.
17. Cass I, Baldwin RL, Varkey T, Moslehi R, Narod SA, Karlan BY. Improved survival in women with BRCA-associated ovarian carcinoma. *Cancer* 2003;97:2187-95.
18. Hastak K, Alli E, Ford JM. Synergistic chemosensitivity of triple-negative breast cancer cell lines to poly(ADP-Ribose) polymerase inhibition, gemcitabine, and cisplatin. *Cancer Res* 2010;70:7970-80.
19. Walsh CS, Ogawa S, Scoles DR, Miller CW, Kawamata N, Narod SA, et al. Genome-wide loss of heterozygosity and uniparental disomy in BRCA1/2-associated ovarian carcinomas. *Clin Cancer Res* 2008;14:7645-51.
20. Goringe KL, Jacobs S, Thompson ER, Sridhar A, Qiu W, Choong DY, et al. High-resolution single nucleotide polymorphism array analysis of epithelial ovarian cancer reveals numerous microdeletions and amplifications. *Clin Cancer Res* 2007;13:4731-9.
21. Li Y, Zou L, Li Q, Haibe-Kains B, Tian R, Li Y, et al. Amplification of LAPTM4B and YWHAZ contributes to chemotherapy resistance and recurrence of breast cancer. *Nat Med* 2010;16:214-8.
22. Harries M, Gore M. Part I: chemotherapy for epithelial ovarian cancer-treatment at first diagnosis. *Lancet Oncol* 2002;3:529-36.
23. Etemadmoghadam D, deFazio A, Beroukhir R, Mermel C, George J, Getz G, et al. Integrated genome-wide DNA copy number and expression analysis identifies distinct mechanisms of primary chemoresistance in ovarian carcinomas. *Clin Cancer Res* 2009;15:1417-27.
24. Clauss A, Ng V, Liu J, Piao H, Russo M, Vena N, et al. Overexpression of elafin in ovarian carcinoma is driven by genomic gains and activation of the nuclear factor kappaB pathway and is associated with poor overall survival. *Neoplasia* 2010;12:161-72.
25. Beroukhir R, Lin M, Park Y, Hao K, Zhao X, Garraway LA, et al. Inferring loss-of-heterozygosity from unpaired tumors using high-density oligonucleotide SNP arrays. *PLoS Comput Biol* 2006;2:e41.
26. <http://biosun1.harvard.edu/complab/dchip/>.
27. Lin M, Wei LJ, Sellers WR, Lieberfarb M, Wong WH, Li C. dChipSNP: significance curve and clustering of SNP-array-based loss-of-heterozygosity data. *Bioinformatics* 2004;20:1233-40.
28. Li C, Beroukhir R, Weir BA, Winckler W, Garraway LA, Sellers WR, et al. Major copy proportion analysis of tumor samples using SNP arrays. *BMC Bioinformatics* 2008;9:204.
29. Rice JC, Ozcelik H, Maxeiner P, Andrusis I, Futscher BW. Methylation of the BRCA1 promoter is associated with decreased BRCA1 mRNA levels in clinical breast cancer specimens. *Carcinogenesis* 2000;21:1761-5.
30. Matros E, Wang ZC, Lodeiro G, Miron A, Iglehart JD, Richardson AL. BRCA1 promoter methylation in sporadic breast tumors: relationship to gene expression profiles. *Breast Cancer Res Treat* 2005;91:179-86.
31. Alsop K, Fereday S, Meldrum C, Defazio A, Emmanuel C, George J, et al. BRCA mutation frequency and patterns of treatment response in BRCA mutation-positive women with ovarian cancer: A report from the Australian Ovarian Cancer Study Group. *J Clin Oncol* 2012;30:2654-63.
32. The Cancer Genome Atlas [homepage on the Internet]. [cited 2011 Oct 27]. Available from: <http://tcga-data.nci.nih.gov/tcga/>.
33. Hennessy BT, Timms KM, Carey MS, Gutin A, Meyer LA, Flake DD II, et al. Somatic mutations in BRCA1 and BRCA2 could expand the number of patients that benefit from poly (ADP ribose) polymerase inhibitors in ovarian cancer. *J Clin Oncol* 2010;28:3570-6.
34. Turner N, Tutt A, Ashworth A. Hallmarks of 'BRCAness' in sporadic cancers. *Nat Rev Cancer* 2004;4:814-9.
35. Konstantinopoulos PA, Spentzos D, Karlan BY, Taniguchi T, Fountzilas E, Francoeur N, et al. Gene expression profile of BRCAness that correlates with responsiveness to chemotherapy and with outcome in patients with epithelial ovarian cancer. *J Clin Oncol* 2010;28:3555-61.
36. Waddell N, Arnold J, Cocciardi S, da Silva L, Marsh A, Riley J, et al. Subtypes of familial breast tumours revealed by expression and copy number profiling. *Breast Cancer Res Treat* 2010;123:661-77.
37. Stephens PJ, McBride DJ, Lin ML, Varela I, Pleasance ED, Simpson JT, et al. Complex landscapes of somatic rearrangement in human breast cancer genomes. *Nature* 2009;462:1005-10.
38. Gu W, Zhang F, Lupski JR. Mechanisms for human genomic rearrangements. *Pathogenetics* 2008;1:4.
39. Mukhopadhyay A, Elattar A, Cerbinskaite A, Wilkinson SJ, Drew Y, Kyle S, et al. Development of a functional assay for homologous recombination status in primary cultures of epithelial ovarian tumor and correlation with sensitivity to poly(ADP-ribose) polymerase inhibitors. *Clin Cancer Res* 2010;16:2344-51.
40. Vang R, Shih le M, Kurman RJ. Ovarian low-grade and high-grade serous carcinoma: pathogenesis, clinicopathologic and molecular biologic features, and diagnostic problems. *Adv Anat Pathol* 2009;16:267-82.
41. Bunting SF, Callen E, Wong N, Chen HT, Polato F, Gunn A, et al. 53BP1 inhibits homologous recombination in Brca1-deficient cells by blocking resection of DNA breaks. *Cell* 2010;141:243-54.
42. Farmer H, McCabe N, Lord CJ, Tutt AN, Johnson DA, Richardson TB, et al. Targeting the DNA repair defect in BRCA mutant cells as a therapeutic strategy. *Nature* 2005;434:917-21.
43. Bryant HE, Schultz N, Thomas HD, Parker KM, Flower D, Lopez E, et al. Specific killing of BRCA2-deficient tumours with inhibitors of poly (ADP-ribose) polymerase. *Nature* 2005;434:913-7.
44. Kuo MT, Chen HH, Song IS, Savaraj N, Ishikawa T. The roles of copper transporters in cisplatin resistance. *Cancer Metastasis Rev* 2007;26:71-83.
45. Komatsu M, Sumizawa T, Mutoh M, Chen ZS, Terada K, Furukawa T, et al. Copper-transporting P-type adenosine triphosphatase (ATP7B) is associated with cisplatin resistance. *Cancer Res* 2000;60:1312-6.
46. Walsh CS, Ogawa S, Karahashi H, Scoles DR, Pavelka JC, Tran H, et al. ERCC5 is a novel biomarker of ovarian cancer prognosis. *J Clin Oncol* 2008;26:2952-8.
47. Birkbak NJ, Eklund AC, Li Q, McClelland SE, Endesfelder D, Tan P, et al. Paradoxical relationship between chromosomal instability and survival outcome in cancer. *Cancer Res* 2011;71:3447-52.
48. De Ligio JT, Velkova A, Zorio DA, Monteiro AN. Can the status of the breast and ovarian cancer susceptibility gene 1 product (BRCA1) predict response to taxane-based cancer therapy? *Anticancer Agents Med Chem* 2009;9:543-9.
49. Swanton C, Nicke B, Schuett M, Eklund AC, Ng C, Li Q, et al. Chromosomal instability determines taxane response. *Proc Natl Acad Sci U S A* 2009;106:8671-6.
50. Kriege M, Jager A, Hoening MJ, Huijskens E, Blom J, van Beurzen CH, et al. The efficacy of taxane chemotherapy for metastatic breast cancer in BRCA1 and BRCA2 mutation carriers. *Cancer* 2012;118:899-907.